Reaction Probabilities for N_2O_5 Hydrolysis on Sulfuric Acid and Ammonium Sulfate Aerosols at Room Temperature

J. H. Hu[†] and J. P. D. Abbatt*

Department of the Geophysical Sciences, The University of Chicago, 5734 S. Ellis Ave., Chicago, Illinois 60637

Received: September 10, 1996; In Final Form: November 11, 1996[⊗]

The uptake coefficients for N_2O_5 hydrolysis have been measured at room temperature on micron-sized aerosols composed of both sulfuric acid aqueous solutions and ammonium sulfate solutions. The measurements have been performed in a laminar flow tube which is coupled to a chemical ionization mass spectrometer for monitoring the concentration of N_2O_5 in the gas phase and an optical particle counter which sizes the aerosols and determines their number density. The aerosols are generated with an ultrasonic nebulizer from aqueous solutions of either sulfuric acid or ammonium sulfate, and their liquid-phase concentration is determined by the relative humidity (RH) set within the flow tube. For both the sulfuric acid and ammonium sulfate aerosols, the reaction probability (γ) is largest for the lowest relative humidities studied: for sulfuric acid aerosols, $\gamma = 0.05-0.06$ for RH = 9−20%, $\gamma = 0.02$ for RH = 90%; for ammonium sulfate aerosols, $\gamma = 0.04-0.05$ for RH = 50−69%, $\gamma = 0.02$ for RH = 83−94%. In the case of ammonium sulfate aerosols, significant reactivity with N_2O_5 is found at relative humidities below the deliquescence point of 80%, consistent with the observation that ammonium sulfate aerosols are readily formed in supersaturated, liquid states.

Introduction

It is now well recognized that the hydrolysis reaction of N_2O_5

$$N_2O_5 + H_2O \rightarrow 2HNO_3 \quad (1)$$

is extremely important in determining the photochemical steady state of the stratosphere, converting reactive nitrogen oxide (NO_x) species over to a longer-lived reservoir species, HNO_3. Indeed, inclusion of reaction 1 in stratospheric models has led to markedly better agreement between predicted ozone depletion rates and those being observed[1] and to a reordering of the catalytic cycles most important in destroying odd oxygen in the lower stratosphere.[2] Given the role of NO_x species in photochemical production of ozone in the lower atmosphere, inclusion of reaction 1 in global tropospheric photochemical models also leads to pronounced changes in the predicted levels of key species such as NO_x, O_3, and OH. For example, with reaction 1 included in a three-dimensional photochemical model, Dentener and Crutzen predict for the free troposphere in the summertime mid-latitudes (45° N, 500 hPa, mid-June) that NO_x and O_3 levels will be only 55 and 90%, respectively, of their values when modeled with gas-phase chemistry alone.[3] Even larger relative changes are predicted for higher latitudes and in the planetary boundary layer. In addition to the importance of reaction 1 on a global scale, it is also well recognized that the reaction plays an important role in the reduction of NO_x levels in polluted urban air.

A major uncertainty in model estimates such as those of Dentener and Crutzen are the appropriate heterogeneous reaction rates, which are determined by a variety of factors including total aerosol surface areas, the chemical composition of tropospheric aerosols, and the corresponding reactivity of N_2O_5 on these surfaces. To address this latter point, we report in this work measurements of the reaction probability of N_2O_5 on both sulfuric acid and ammonium sulfate aerosols using the aerosol flow tube technique. Motivations for this study are twofold. First and foremost, although this reaction has now been studied extensively under stratospheric conditions (i.e., low temperatures and sulfuric acid compositions of 50−80 wt %), notably fewer experiments have been performed on dilute sulfuric acid surfaces and on surfaces other than sulfuric acid. In particular, given the high relative humidities encountered frequently in both the boundary layer and free troposphere, the composition of tropospheric sulfate aerosols may be significantly more dilute than those encountered in the stratosphere. In addition, although stratospheric aerosols are believed to be predominantly composed of sulfuric acid and water, in the troposphere there is substantial evidence that ammonia plays a significant role in neutralizing pure sulfuric acid aerosols.[4] In continental regions in the boundary layer, sulfate aerosols can be fully neutralized in the form of ammonium sulfate, $(NH_4)_2SO_4$, whereas in the free troposphere remote from continental influence, the aerosols are likely to be more acidic.[5−7]

A second motivation for this study is that reaction 1 on concentrated sulfuric acid surfaces is by far the most frequently studied heterogeneous reaction,[8] making it the best chemical system to use to evaluate the performance of an aerosol flow tube experimental technique we have been developing in our laboratory. For a number of reasons, aerosol flow tubes are being increasingly employed for heterogeneous studies of this type.[9−12] In particular, for reaction probabilities of roughly 0.1 and smaller measured on micron-sized aerosols, there is the need for only a relatively small correction to observed uptake coefficients for the effects of gas-phase diffusion. On the other hand, the coated-wall flow tube technique is largely inoperable if a few Torr of water vapor is present in the flow tube because gas-phase diffusion becomes rate limiting for all but the smallest uptake coefficients. A second advantage, illustrated by Hanson and Lovejoy, is the ability of experiments performed on aerosols

* To whom correspondence should be sent.
[†] School of Earth and Atmospheric Sciences, Georgia Institute of Technology, Atlanta, GA 30332.
[⊗] Abstract published in *Advance ACS Abstracts,* January 1, 1997.

S1089-5639(96)02743-0 CCC: $14.00

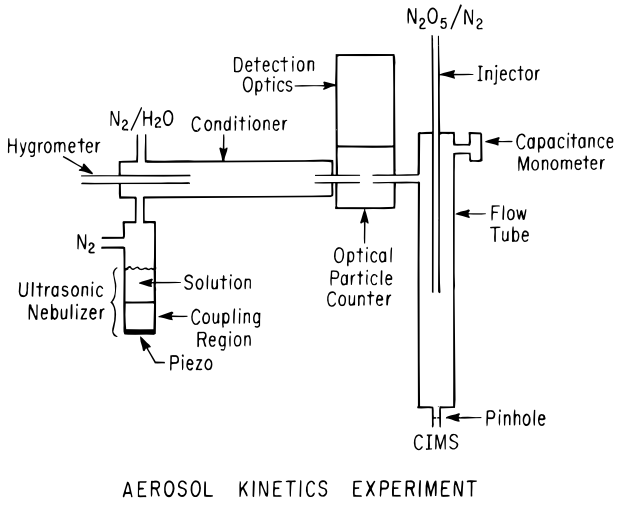

Figure 1. Schematic of experimental apparatus.

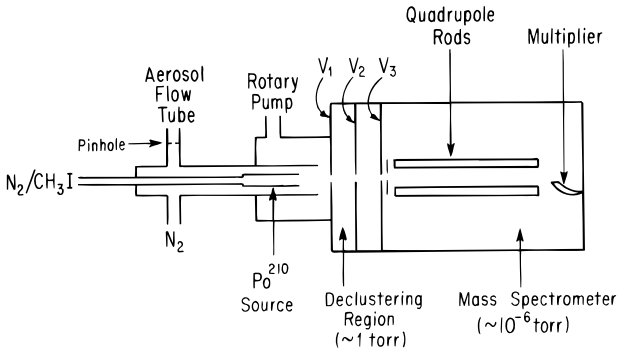

Figure 2. Schematic of chemical ionization mass spectrometer.

to study the dependence of observed uptake coefficients upon aerosol size.[13]

Although the general approach—the measurement of the loss of a gas-phase species upon aerosol distributions of varying total surface area—is similar to other aerosol flow tube experiments, the instrumental techniques we are using are somewhat different from those used previously. In particular, the aerosol flow tube configuration used in this work employs a laminar flow tube, coupled to a chemical ionization mass spectrometer for monitoring the gas-phase composition, to an optical particle counter for the determination of aerosol size and number density, and to an ultrasonic nebulizer aerosol source. Results that agree well with previous measurements are reported for the room temperature uptake coefficients of N_2O_5 on relatively concentrated sulfuric acid aerosols, i.e., 59−66 wt %. In order to better model tropospheric sulfate aerosol compositions, we also report measurements for both more dilute sulfuric acid compositions (17 and 40 wt %) and a variety of ammonium sulfate aerosol compositions. Because these measurements have been performed over a wide range of aerosol compositions using the same experimental technique, this data set allows us to accurately assess the dependence of the overall reaction probability upon the water content of sulfate aerosols.

Experimental Section

Aerosol Generation. The overall experimental configuration is shown in Figures 1 and 2. Aerosols are generated from sulfuric acid and ammonium sulfate solutions by an in-lab-built ultrasonic nebulizer driven by a 2.5 cm diameter piezocrystal. A 5 cm long coupling region, filled with water and sealed with Teflon-coated Viton O-rings and a thin Teflon sheet, isolates the solution being nebulized from the metallic coating of the piezocrystal. A small flow of N_2 gas (10−50 sccm) carries the aerosols into a 47 cm long, 3 cm i.d. conditioning region where they have a residence time of typically 10 s. We can vary the aerosol number density in the conditioner either by varying the voltage applied to the crystal or by changing the flow of the N_2 carrier gas through the nebulizer.

The aerosols adjust their composition in the conditioner to the ambient relative humidity, which is set by adding both a dry flow of N_2 and a water-saturated flow of N_2 coming from a bubbler kept at constant temperature. The small amount of water vapor from the moist flow of N_2 coming from the nebulizer is also taken into consideration. The total N_2 flow from these three sources is about 2000 sccm. From the error estimates in the flows and temperatures of the bubbler, we estimate the errors in the relative humidity in the conditioner to be ±1% and no larger than ±2%. Indeed, during the ammonium sulfate experiments, we compared the relative humidity calculated in this manner to that monitored by a dew point hygrometer (Fisher Scientific) and found that the two were in agreement to this degree. Assuming that the aerosols are in equilibrium with the ambient flow conditions, this potential error in the relative humidity corresponds to an inaccuracy of no more than ±2 wt % in the composition of the aerosols, where the relationship between the relative humidity and the composition of the aerosols is taken from refs 14 and 15.

Aerosol Surface Area Determination. After the conditioner, the flow containing the aerosols passes through a 6 mm o.d., 12 cm long Pyrex tube which is inserted into the detection region of a commercially built optical particle counter (Particle Measuring Systems, Inc., No. SSIP-S2). The optical particle counter uses a 780 nm polarized light source which sits at right angles to the scattered-light collection optics and detection photodiodes; i.e., the laser beam is perpendicular to the page in Figure 1. The intersection of the laser beam and collection optics defines a detection volume that was designed to be particularly small so as to keep coincidence errors negligible for aerosol number densities below $10^5/cm^3$. Using a calibration performed by Particle Measuring Systems with latex and glass spheres of known size, aerosols are sized based on the intensity of the scattered signals from individual aerosols which enter the detection volume. The lower detection limit for aerosol size is 0.2 μm diameter, the upper limit is 20 μm, and aerosols are classified into one of 31 channels between these two limits. Using latex and glass spheres of 0.50, 1.0, 2.0, and 9.6 μm diameter (Duke Scientific), we routinely check that the calibration of the instrument is good to at least one size channel, or roughly 10−15% sizing accuracy.

Scattered light signals per unit time are converted into aerosol number densities via knowledge of the detection volume sampled per unit time, which is defined by both the optical configuration and by the flow velocity in the detection volume. Assuming fully developed laminar flow in the 6 cm o.d. intake tube, we take this velocity to be twice the bulk velocity in the tube. Using a Pitot−static probe with a small sampling inlet (1.0 mm) which is coupled to a differential capacitance manometer (MKS-220CD, 1 Torr full scale), velocities measured in the aerosol detection region agree with the velocities calculated from the bulk flow to within 4%. In general, the instrument has been calibrated to have better than 10% counting accuracy (J. Knollenberg, Particle Measuring Systems, personal communication).

Typical aerosol number density and surface area density distributions for ≈60 wt % H_2SO_4 aerosols are shown in Figure 3. Two polydisperse aerosol distributions are clearly being

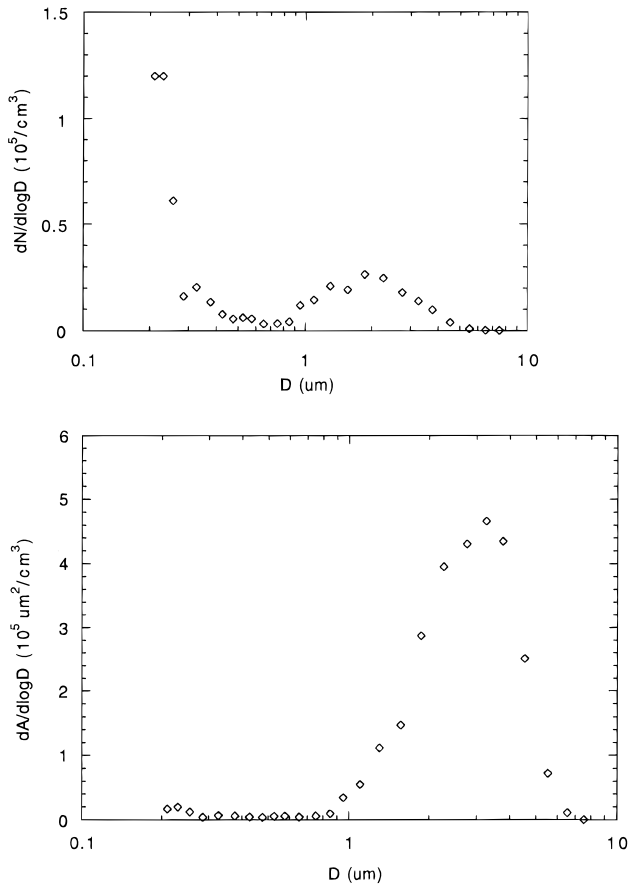

Figure 3. Typical aerosol number density (a, top) and surface area (b, bottom) distributions observed by the optical particle counter for sulfuric acid aerosols at a relative humidity of 20%.

generated by the nebulizer: a distribution with large aerosols ($\approx$1−6 μm in diameter) characteristic of mechanical formation mechanisms and a distribution of much smaller aerosols in the submicron range. Although a number of quite small aerosol particles (<0.3 μm diameter) are generated by the nebulizer source, they do not contribute significantly to the overall aerosol surface area in the flow tube. For example, aerosols smaller than 0.3 μm typically contribute less than 1% of the measured aerosol surface area in the flow. Typical number densities of the large particles present in the flow tube for kinetics studies were $3 \times 10^3-2 \times 10^4$ aerosols/cm^3, and corresponding aerosol surface areas were $3 \times 10^4-7 \times 10^5$ cm^2/cm^3. The peak of the surface area distribution was typically between 2 and 4 μm diameter.

In light of the importance of accurately determining aerosol sizes and number densities (and thus, total aerosol surfaces areas and volumes) in kinetics experiments of this type, we have determined the sensitivity of the instrument to total aerosol volumes using a calibration approach which is independent of the optical particle counter. In particular, the approach we have taken is to establish a flow of either sulfuric acid or ammonium sulfate aerosols of known composition through the counter under flow conditions used in the kinetics experiments. All the aerosols passing through the counter within a measured time period are collected in an aqueous trap located immediately downstream of the counter. After the collection period, the electrical conductivity of the aqueous trap is then measured. We believe that the trap is 100% efficient at aerosol collection because we placed on one occasion a second trap in series with the first and recorded no conductivity increase in the second trap. Although there is the possibility that there were aerosol losses between the counter and the trap, we kept the length of tubing between the two to the minimum ($\approx$5−10 cm long), and consequently we believe the losses to be minor.

The number of moles of either sulfuric acid or ammonium sulfate which flowed through the optical particle counter during the collection period is then calculated according to

$$\text{moles solute from electrical conductivity} = (CV_t)/\Lambda^o \quad (2)$$

where C is the measured electrical conductivity (in μmho/cm), V_t is the volume of the aqueous trap (in cm^3), and Λ^o is the molar conductivity for the solute of interest (in (μmho cm^2)/mol).[16] Typical conductivities measured were on the order of hundreds of μmho/cm for a collection time of 5 min, whereas the background conductivity of the distilled/deionized water in our laboratory is about 1 μmho/cm.

Figure 4 is a typical aerosol volume calibration plot where moles of solute determined from the conductivity measurements is plotted against moles of solute determined from the optical particle counter during the aerosol trapping period:

$$\text{moles solute from optical particle counter} = (V_d \varphi t \rho \text{ wt \%})/\text{MW} \quad (3)$$

where V_d is the average aerosol volume measured by the counter (in cm^3/cm^3), φ is the carrier gas rate (in cm^3/min), t is the trapping time (in minutes), ρ is the density of the aerosol (in g/cm^3), wt % is the percentage weight composition of the aerosol, and MW is the molecular weight of the solute of interest.

For all the calibrations which we have performed, plots such as these are highly linear which is indicative that the counter is responding linearly to typical total aerosol volumes used in this work. For aerosols of 66 wt % sulfuric acid, the slope of this plot is relatively close to unity, whereas for more dilute solutions, such as 17 wt % sulfuric acid shown in Figure 4, the slopes are somewhat smaller than unity. The change in the counter response as a function of aerosol composition is a well-known observation, due to the smaller refractive index of the more dilute aerosols.[17] That is, the smaller refractive index leads to a reduction in the ability of the more dilute aerosols to scatter light when compared to more concentrated aerosols of higher refractive index. Because the counter is undersizing the dilute aerosols, we use plots such as Figure 4 to calibrate the counter response by correcting the observed aerosol size by a factor equal to the reciprocal of the slope of these plots to the one-third power.

During the course of running a full kinetics experiment, we monitor a small buildup of aerosol material on the walls of the flow tube immediately opposite the inlet from the optical particle counter. This is most likely due some of the aerosols failing to follow the flow around the 90° bend. We performed an extensive set of experiments with the electrical conductivity technique to determine, for constant flow and aerosol compositions, the aerosol volumes determined at the outlet of the kinetics flow tube relative to the volumes determined by trapping at the outlet of the optical particle counter. Aerosol volumes were consistently lower at the flow tube outlet by an average of 15 $\pm$ 5%. Consequently, for the kinetics experiments described below, we have corrected our total aerosol surface areas by this factor to account for the loss of aerosols at the top of the flow tube. No kinetics measurements were made in the region of the flow tube where aerosol was seen to be accumulating on the wall.

The calibrations performed with the electrical conductivity technique show very high precision and are quite reproducible (to at least 10%) over extended time periods of months. Because

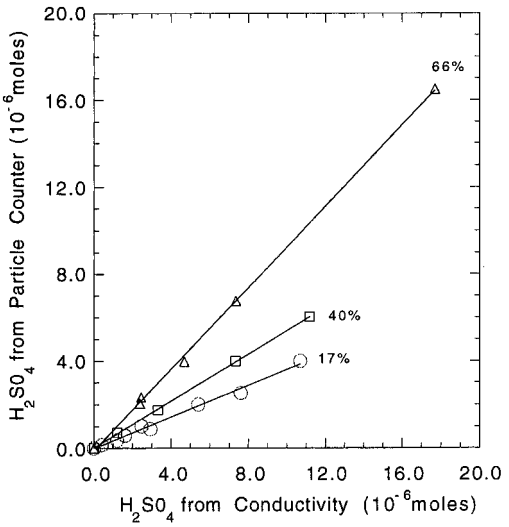

Figure 4. Optical particle counter calibration plot using electrical conductivity analysis of collected aerosols (see text).

this approach is directly measuring total aerosol volumes which are flowing through the flow tube, we estimate that systematic errors in total aerosol volumes are no larger than ±25%. The systematic errors in total aerosol surface areas will be equal to or smaller than this estimate.

Delivery of N_2O_5 and Aerosols to the Kinetics Flow Tube. The aerosol flow passes from the optical particle counter to the 3.0 cm i.d. reaction flow tube which is oriented vertically, at right angles to the conditioner and the flow path through the optical particle counter. For the majority of the studies reported here the reaction flow tube was 90 cm long whereas for some of the initial studies, a shorter flow tube of 48 cm length was used. The total pressure in the flow tube was 750 ± 10 Torr, and the bulk flow velocity was roughly 5 cm/s. The terminal fall velocity of the largest aerosols used in this work was less than 2% of the carrier gas bulk velocity.

N_2O_5 was synthesized at room temperature by oxidizing NO_2 with O_3 produced from O_2 carrier gas and a UV photolysis source (Jelight Co., PS-3001-30). To remove H_2O vapor from the O_2 carrier gas, a P_2O_5 trap was placed immediately upstream of the ozonizer and reaction tube. N_2O_5 was injected into the flow at concentrations of $5 \times 10^{12}-1 \times 10^{14}$ molecules/cm^3 via a 6 mm o.d. movable injector by passing a carrier gas of 30−50 sccm of N_2 through a trap containing solid N_2O_5 which was kept at −50−70 °C. To reduce the formation of HNO_3 in the trap, the carrier gas for the N_2O_5 passed through a P_2O_5 trap prior to entering the N_2O_5 trap. We checked that the N_2 carrier gas was saturated with the vapor pressure of N_2O_5 at the temperature of the trap by passing the flow through a 50 cm long absorption cell and by measuring the absorption signal at 254 nm due to N_2O_5. The partial pressure of N_2O_5 measured by the absorption measurements was within 7% of that calculated by assuming the flow was saturated with N_2O_5. The walls of the flow tube were coated with halocarbon wax to minimize N_2O_5 wall loss, and they were washed and dried between kinetics runs.

N_2O_5 Detection. N_2O_5 was detected as NO_3^- by chemical ionization mass spectrometry (CIMS) using the I^- reagent ion: $I^- + N_2O_5 \rightarrow NO_3^- + INO_2$. This detection scheme has been used before to selectively monitor N_2O_5 in the presence of HNO_3, which is believed to not react with I^-.[18,19] As shown in Figure 2, the entire flow from the aerosol reaction tube passes into the CIMS source where it mixes with a much larger flow of N_2 at a pressure of 120 Torr. The pressure drop from the 750 Torr aerosol flow tube to the lower pressure CIMS source occurs across a pinhole in a Teflon sheet mounted between the two flow tubes. In the CIMS reactor, 3.5 SLM of N_2 pass through a radioactive (Po-210) ion source (NRD Inc.) mounted at the end of a 6 mm o.d. stainless steel tube. An additional 7 SLM passes around the outside of the ion source. I^- ions, generated by passing trace amounts of CH_3I (Aldrich) over the Po-210 source, react with N_2O_5 during a 10 ms time period defined by the overall flow and the distance between the end of the ion source and the sampling pinhole to the mass spectrometer. Ions generated at high pressure pass through three stages of differential pumping en route to an Extrel quadrupole mass spectrometer. The pinholes that separate the different pumping stages are biased with voltages of −200, −40, and −15 V for the high-, middle-, and low-pressure stages, respectively. The first stage, at 1 Torr pressure and pumped with a rotary pump, was found to be a very efficient declustering region for ion−water clusters which readily form in the expansion of high-pressure flows containing high partial pressures of water vapor.[20] With this declustering region in operation, we observe no water clusters in the final mass spectrum, whereas without this region, the mass spectrum was very much more complicated. The second stage of the differential pumping, evacuated with a diffusion pump, is at 1×10^{-3} Torr, and the final stage, containing the quadrupole mass spectrometer and pumped with a turbomolecular pump, is at 1×10^{-5} Torr.

For some of the original studies on 40 and 59 wt % sulfuric acid aerosols, the overall sensitivity of the CIMS system was relatively low, requiring the use of high concentrations of N_2O_5 ($\approx 1 \times 10^{14}$ molecules/cm^3) in the aerosol flow tube. However, for all the other studies reported here, the geometry of the CIMS source was altered slightly, and the sensitivity was considerably higher. For these studies, a concentration of 7×10^{12} molecules/cm^3 of N_2O_5 in the aerosol flow tube was used. This corresponds to a concentration of 1.7×10^{11} molecules/cm^3 in the CIMS flow tube, and it gives rise to a signal of roughly 200 counts/s. Although the reaction between I^- and HNO_3 is endothermic and not expected to proceed, we nevertheless observed a weak signal arising from HNO_3 in the presence of I^- under certain conditions. Similar behavior has been observed by other workers.[21] We believe that the HNO_3 arises principally as a product of reaction 1 because in separate experiments with an electron-impact mass spectrometer we have quantified the HNO_3 partial pressure impurity arising from our N_2O_5 samples to be no more than 50% of the N_2O_5 signal. Thus, the HNO_3 background of ≈5−10 counts/s was determined by decaying away all the N_2O_5 in the flow tube by operating under conditions of high surface area and long reaction times; i.e., the injector was pulled fully out. Simple first-order kinetics analysis predicts that this background will be essentially constant compared to the relative changes in the N_2O_5 signal for the reaction times and first-order rate constants characteristic of our experiment.

For these conditions, the detection limit (S/N = 1) for N_2O_5 was roughly 3×10^9 molecules/cm^3 in the CIMS flow tube, corresponding to 1×10^{11} molecules/cm^3 in the aerosol flow tube. These are likely to be upper limits to the detection limit because we are assuming that there is no decay of N_2O_5 along the Teflon lines connecting the N_2O_5 trap and the flow tube. For all the kinetics studies, the I^- signal was on the order of 200 000 counts/s, and it was stable as the N_2O_5 concentration changed during a decay.

Results

Typical decays of N_2O_5 as a function of injector distance for a variety of aerosol surface areas for 17 wt % sulfuric acid

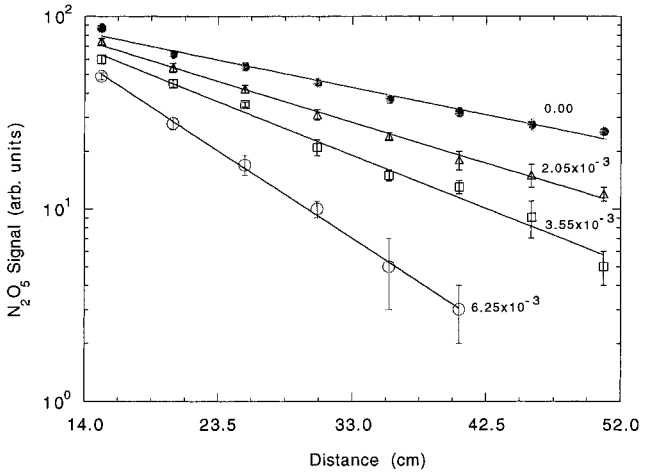

Figure 5. Semilog plot of N_2O_5 signal as a function of injector position for a variety of 17 wt % sulfuric acid aerosol surface areas and for wall loss.

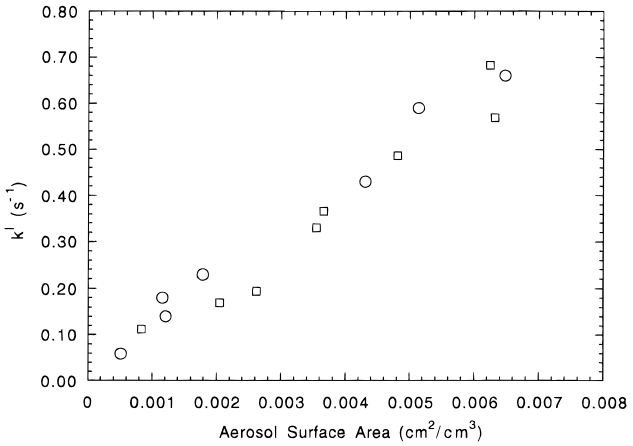

Figure 6. First-order rate constant for N_2O_5 reaction due to aerosol reaction as a function of total aerosol surface area for 17 wt % sulfuric acid aerosols: squares, data from long flow tube; circles, data from short flow tube.

aerosols are shown in Figure 5. Within experimental error, the decays are first order. Note that there is a loss of N_2O_5 due to wall reaction in the absence of aerosols, where the wall decay was measured immediately after performing kinetics experiments with aerosols in the flow tube. It was observed that larger wall losses were somewhat correlated with higher relative humidities in the flow tube, with observed first-order wall-loss rate constants of roughly 0.1 s^{-1}.

The Reynolds number for flow conditions in this work was typically between 90 and 100. As a result, the entrance length which is conventionally used to describe the point at which fully developed laminar flow is developed, i.e., the distance at which the center line velocity of the flow reaches 1.99 times the value of the bulk velocity, is on the order of 16 cm.[22] For the longer flow tube used here, which was employed for all the ammonium sulfate studies and for the studies of 17 and 67 wt % sulfuric acid, all decays were monitored starting at a distance of 20 cm from the downstream end of the flow tube. That is, laminar flow was fully established for the entire length of the decay. For the shorter flow tube, which was employed for the 40 and 59 wt % sulfuric acid studies, we used only a 10 cm entrance length. However, given the asymptotic nature by which laminar flow approaches a steady-state velocity profile, we feel confident that this was sufficient length to allow a close approximation to fully developed flow to be attained. In particular, it can be calculated for our flow conditions that the center line velocity after a 10 cm entrance length will already be 1.94 as large as the bulk flow velocity.[22]

These entrance lengths not only allow the flow to approximate fully developed laminar conditions, but they also give time for mixing of N_2O_5 from the injector into the bulk flow. The time for mixing to occur via molecular diffusion to a level where there are no more than 5% inhomogeneities in the flow occurs in a distance of roughly 15 cm for our flow conditions.[23] It is likely that mixing into the bulk in fact occurs much faster than this via turbulent mixing processes, given the presence of the injector and the fact that N_2O_5 is being injected into the flow tube carrier gas.

The injector distances shown in Figure 5 are converted into reaction times using the bulk flow velocity and a standard correction, developed by Brown,[24] to account for non-plug-flow conditions. The overall N_2O_5 loss observed in the presence of aerosols, along with the loss of N_2O_5 in the absence of aerosols due to wall reaction, were used as input for this calculation. The first-order-loss rate coefficients, k^I, due to aerosol loss alone for 17 wt % sulfuric acid aerosols are plotted in Figure 6 versus the average total aerosol surface area measured during the decay. Two sets of data, one set obtained with the long flow tube and an additional one with the short flow tube, are shown in Figure 6. As indicated below, for the scatter within the individual sets of measurements, the two sets of data yield statistically indistinguishable average values of the uptake coefficient. Thus, we feel confident in reporting uptake coefficients performed using both the longer and shorter flow tubes. The scatter in plots such as Figure 6 is believed to arise from a number of sources including variable wall losses during a set of measurements, random errors in the experimental first-order decays, and variability in the total aerosol surface area during the decay. With respect to this latter point, typical 1σ precisions for the surface area measured during a decay were on the order of $\pm 5\%$.

To convert first-order rate constants to gas−liquid uptake coefficients, eq 4 is used to connect the regime where gas-phase loss is in the kinetic limit to that where it is in the gas-phase diffusion limit:[25]

$$k_i^{\mathrm{r}} = \frac{\gamma N_i \pi d_i^{\,2} \upsilon}{4 + \dfrac{3\gamma(1 + 0.38K_n)}{K_n(1 + K_n)}} \tag{4}$$

where k^I_i is the first-order rate constant due to aerosol size d_i, υ is the mean molecular velocity for N_2O_5, and K_n, the Knudsen number, equals $6D_g/d_i\upsilon$. D_g is the diffusion coefficient for N_2O_5 in the carrier gas. Because eq 4 assumes a monodisperse aerosol distribution, we have evaluated the majority of our data by taking the size of the aerosols, d_i, to be at the maximum of the surface area density distribution for the large aerosols, i.e., those larger than about 0.5 μm. Since our aerosol distribution of large aerosols is clearly not monodisperse, we have validated this assumption, by also performing the full calculation for a few test cases using a measured aerosol size distribution. In particular, for these cases we determine the uptake coefficient by solving eq 5

$$k^{\mathrm{I}} = \sum_i k^{\mathrm{I}}{}_i \tag{5}$$

for the uptake coefficient, where each individual k^I_i is calculated from eq 4 for every aerosol size measured by the optical particle counter. The uptake coefficient calculated in this manner, which takes into account the polydisperse nature of our aerosols, agrees with the uptake coefficient calculated by assuming a monodisperse distribution to better than 5%.

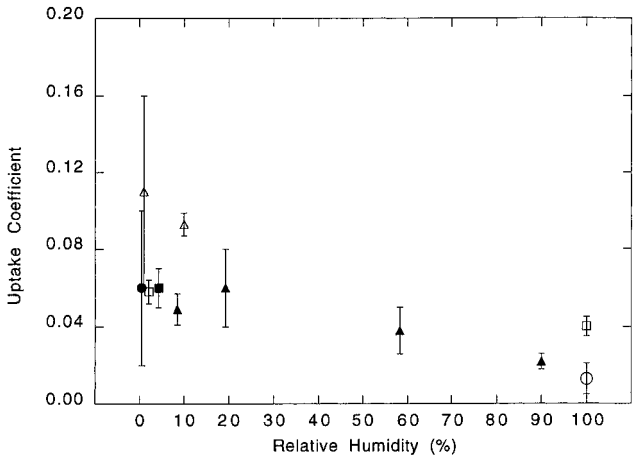

Figure 7. Uptake coefficient for N_2O_5 on sulfuric acid aqueous solutions and water surfaces as a function of relative humidity: filled triangles, this work (297 K); filled circle, Fried et al.[10] (293 K); open triangles, Mozurkewich and Calvert[9] (293 K); open squares, Van Doren et al.[30] (282 K); filled square, Lovejoy and Hanson[12] (298 K); open circle, George et al.[31] (277 K).

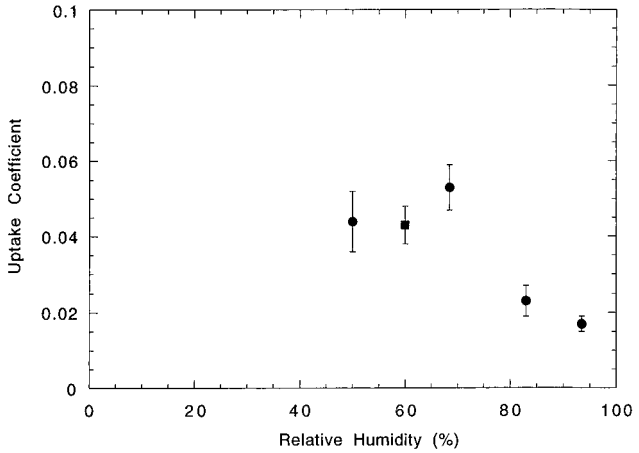

Figure 8. Uptake coefficient for N_2O_5 on ammonium sulfate aerosols as a function of relative humidity: filled circle, this work (297 K); filled square, Mozurkewich and Calvert[9] (293 K).

For this work we have used a diffusion coefficient for N_2O_5 in the carrier gas of 0.10 cm^2/s for our total pressures of 750 Torr in the flow tube. This value was calculated using standard Lennard-Jones parameters taken from refs 26 and 27. The calculated value for the diffusion coefficient is not significantly affected by the presence of variable amounts of water vapor in the flow. The size of the diffusion correction relative to the uptake coefficients which would be calculated in the kinetic limit is on the order of 10−50%, depending upon the size of the aerosols and the size of the uptake coefficient.

The uptake coefficients which we report for N_2O_5 hydrolysis on a range of compositions of sulfuric acid and ammonium sulfate aerosols are given in Figures 7 and 8 and in Tables 1 and 2. The errors listed in the figures and tables reflect 1σ precisions. Potential systematic errors could arise from a variety of sources including the treatment of non-plug-flow conditions in the flow reactor, the correction made to account for gas-phase diffusion, and the measurement of the aerosol surface areas in the flow tube. Although we have no a priori method to test the Brown correction procedure for non-plug-flow conditions,[24] it can be noted that Lovejoy and Hanson have performed uptake coefficient measurements using pulsed injection of N_2O_5 to experimentally determine reaction times.[12] These workers have found that the pulsed studies agree with those from the more conventional steady-state experiments to 4%,

TABLE 1: Uptake Coefficients for N_2O_5 on H_2SO_4 Aqueous Aerosols

RH (%)	H_2SO_4 compn (wt %)	uptake coeff[a]	no. of expts
90.0	17	0.023 ± 0.004[b]	15
		0.021 ± 0.004[c]	8
		0.024 ± 0.004[d]	7
58.5	40	0.038 ± 0.012[d]	5
19.5	59	0.060 ± 0.020[d]	7
8.5	66	0.050 ± 0.008[c]	5

[a] Data at 297 ± 1 K. [b] Data from both short and long flow tubes. [c] Data from long flow tube. [d] Data from short flow tube.

TABLE 2: Uptake Coefficients for N_2O_5 on $(NH_4)_2SO_4$ Aqueous Aerosols

RH (%)	$(NH_4)_2SO_4$ compn (wt %)	uptake coeff[a]	no. of expts
93.5	20	0.017 ± 0.002	5
83.0	40	0.023 ± 0.004	5
68.5	60	0.053 ± 0.006	7
50.0	80	0.044 ± 0.008	5

[a] Data at 297 ± 1 K.

thus validating the correction procedure for non-plug-flow conditions to this degree of accuracy. Similarly, we have no method to check the accuracy of the gas-phase diffusion correction, but the dominant source of error in this regard is most likely to arise from incorrectly determining the peak of the aerosol surface area distribution. Assuming an inaccuracy of 10% in our ability to size the aerosols, this corresponds to a relatively small potential error of 2% for uptake coefficients of 0.02 and 5% for uptake coefficients of 0.05. The final source of potential systematic error, which we believe to be on the order of ±25% as described above, arises from the measurement of the total aerosol surface areas in the flow tube.

It should be noted that there is the possibility that HNO_3 formed as a result of reaction 1 will be strongly partitioned from the gas phase to the aerosol, thus affecting the composition of the aerosols being studied. This is of most concern to the ammonium sulfate studies because the Henry's law solubility of HNO_3 into such solutions is extremely high.[28] For the maximum gas-phase concentrations of HNO_3 expected to be in the flow tube for a gas-phase concentration of N_2O_5 of 7×10^{12} molecules/cm^3, it is calculated that the maximum dissolved concentration of HNO_3 which could arise in the aerosols is 0.3 M, assuming the nitric acid is fully partitioned to the condensed phase. This liquid-phase concentration estimate is valid only for a few runs where small total aerosol volumes were used, $\approx 8 \times 10^{-8}$ cm^3/cm^3. Most of the kinetics studies used significantly larger aerosol volumes, and the estimated concentration of HNO_3 in the aerosols is thus smaller than 0.3 M. Along the same line of thought, the partial pressures of N_2O_5 used in the 40 and 59 wt % sulfuric acid studies were very high ($\approx 1 \times 10^{14}$ molecules/cm^3), which will have produced high concentrations of HNO_3 in the gas phase. However, the Henry's law constant for HNO_3 in sulfuric acid solutions of this composition is sufficiently low that very little HNO_3 is expected to be have been partitioned to the aerosols.[29] One advantage of using large aerosols in this experiment is that aerosol volumes are correspondingly high, making these potential interferences of relatively minor importance.

Discussion

Confidence in the present set of uptake coefficient measurements comes from comparison to other results in the literature for sulfuric acid at low relative humidities. In particular, other measurements of the N_2O_5 hydrolysis reaction probability on either sulfuric acid or ammonium sulfate surfaces which were

performed relatively close to room temperature are included in Figures 7 and 8. Included in the comparison are data from a variety of experimental techniques: aerosol flow tube measurements from Mozurkewich and Calvert,[9] Fried et al.,[10] and Lovejoy and Hanson[11,12] and droplet train experiments of Van Doren et al.[30] and George et al.[31] Agreement for the sulfuric acid studies at low relative humidities is quite good. In particular, our results at 8.5 and 19.5% relative humidity fall within the error limits of the studies of Van Doren et al., Fried et al., and Lovejoy and Hanson. It should be noted that the Fried et al. experiment represents the latest version of the Mozurkewich and Calvert aerosol kinetics study, which initially reported the larger uptake coefficients on sulfuric acid shown in the figures.

At high relative humidities, the N_2O_5 uptake coefficient has not previously been measured on sulfuric acid solutions. However, for comparison sake, we have included in Figure 7 results measured on pure water surfaces by both Van Doren et al. and George et al. at 282 and 277 K, respectively. From the figure it appears as though uptake coefficients on dilute sulfuric acid solutions are similar to those measured on water surfaces. It should be noted that both the Van Doren et al. and George et al. studies report a substantial negative temperature dependence to the uptake coefficient on water (for example, from Van Doren et al.[30] $\gamma^{N_2O_5} = 0.040 \pm 0.005$ at 282 K and 0.061 ± 0.004 at 271 K), so a comparison to our measurements performed at 297 K on dilute sulfuric acid may not be entirely appropriate.

The most intriguing aspect of the data in Figure 7 is that the N_2O_5 uptake coefficient is somewhat higher at lower relative humidities than at high relative humidities. This behavior is distinctly different from that displayed by $ClONO_2$ uptake on sulfuric acid solutions, which shows a strong trend in the opposite direction.[8] The relative independence of the uptake coefficient upon acid composition has been observed previously,[8,32] and it implies that water does not play a direct, reactive role in the rate-determining step for the reaction. Rather, the rate-determining step for the reaction appears to be either that involved in the ability of the surface to accommodate N_2O_5 or that involved in the dissociation into NO_2^+ and NO_3^-. In aqueous solution, both NO_2^+ and NO_3^- will readily form HNO_3, the end products of the reaction. At this point it is unknown which step is rate-determining or whether the two steps are coupled as one concerted process.

For ammonium sulfate aerosols, there is only one other measurement in the literature, that of Mozurkewich and Calvert.[9] As shown in Figure 8, the agreement between the present study and one experiment taken from reference 9 is very good. The most interesting aspect of these results is the relatively high reactivity of N_2O_5 at relative humidities well below the deliquescence point of $(NH_4)_2SO_4$ of 79.5%.[4] It has been shown by Tang and co-workers using an electrodynamic trap that liquid ammonium sulfate aerosols do not lose their water to form a dry crystal at the deliquescence point, but that they remain in a supersaturated, liquid state until relative humidities reach roughly 40%, at which point they make a transition to a solid crystal.[33] In our lab, using an FTIR spectrometer coupled to an aerosol absorption cell we have observed similar behavior by monitoring liquid water infrared absorption features in micron-sized ammonium sulfate aerosols.[34] These absorption features persist in the spectra as the relative humidity is ramped down and only disappear at relative humidities below 40%. This propensity to form supersaturated solutions is likely to occur in the atmosphere, and it will have a direct effect upon the reactivity of the aerosols since dry ammonium sulfate has been found to be highly unreactive to N_2O_5 by Mozurkewich and Calvert:[9] e.g., $\gamma < 0.003$ for relative humidity of 25%. Similarly, in some of our ammonium sulfate experiments we lowered the relative humidity below 40% under conditions of high aerosol surface area, and we observed very small loss of N_2O_5, corresponding to $\gamma \leq 0.01$. Although this reaction probability limit is highly uncertain because the particles are solid under these conditions and our aerosol scattering calibrations are not necessarily appropriate, it nevertheless appears as though N_2O_5 is quite unreactive on dry particles.

For photochemical modeling within the boundary layer these results indicate that the reaction probability will be dependent upon the ambient relative humidity. For example, for sulfuric acid aerosols close to room temperature, the appropriate reaction probability for the N_2O_5 hydrolysis is on the order of 0.025 for high relative humidity conditions, e.g., those corresponding to sulfuric acid aerosols of ≈20 wt % composition. For lower relative humidities and more concentrated sulfate aerosols, the data support a somewhat larger reaction probability near 0.05.

Acknowledgment. This work has been supported financially by both the Atmospheric Chemistry Program at the National Science Foundation and the SASS Program at NASA. The authors thank John Seeley for guiding us in the design of our CIMS instrument, Greg Huey for suggesting the use of the Po-210 ion source, and Dennis O'Brien for writing some of the data acquisition software.

References and Notes

(1) World Meteorological Organization, *Scientific Assessment of Ozone Depletion: 1994*, WMO Report No. 37, 1995.

(2) Wennberg, P. O.; Cohen, R. C.; Stimpfle, R. M.; Koplow, J. P.; Anderson, J. G.; Salawitch, R. J.; Fahey, D. W.; Woodbridge, E. L.; Keim, E. R.; Gao, R. S.; Webster, C. R.; May, R. D.; Toohey, D. W.; Avallone, L. M.; Proffitt, M. H.; Loewenstein, M.; Podolske, J. R.; Chan, K. R.; Wofsy, S. C. *Science* **1994**, *266*, 398.

(3) Dentener, F. J.; Crutzen, P. J. *J. Geophys. Res.* **1993**, *98*, 7149.

(4) Warneck, P. *Chemistry of the Natural Atmosphere*, Academic Press: San Diego, 1988 and references therein.

(5) Huebert, B. J.; Lazrus, A. L. *J. Geophys. Res.* **1980**, *85*, 7, 337.

(6) Ferek, R. J.; Lazrus, A. L.; Haagenson, P. L.; Winchester, J. W. *Environ. Sci. Technol.* **1983**, *17*, 315.

(7) Whelpdale, D. M.; Keene, W. C.; Hansen, A. D. A.; Boatman, J. *Glob. Biogeochem. Cycles* **1987**, *1*, 357.

(8) For example: DeMore, W. B.; Sander, S. P.; Golden, D. M.; Hampson, R. F.; Kurylo, M. J.; Howard, C. J.; Ravishankara, A. R.; Kolb, C. E.; Molina, M. J. *Chemical Kinetics and Photochemical Data for Use in Stratospheric Modeling, Evaluation Number 11*, JPL Publication 94-26, Pasadena, 1994.

(9) Mozurkewich, M.; Calvert, J. G. *J. Geophys. Res.* **1988**, *93*, 15889.

(10) Fried, A.; Henry, B. E.; Calvert, J. G.; Mozurkewich, M. *J. Geophys. Res.* **1994**, *99*, 3517.

(11) Hanson, D. R.; Lovejoy, E. R. *Geophys. Res. Lett.* **1994**, *21*, 2401.

(12) Lovejoy, E. R.; Hanson, D. R. *J. Phys. Chem.* **1995**, *99*, 2080.

(13) Hanson, D. R.; Lovejoy, E. R. *Science* **1995**, *267*, 1326.

(14) Zaytsev, I. D.; Aseyev, G. G. *Properties of Aqueous Solutions of Electrolytes*; CRC Press: New York, 1992.

(15) Perry, R. H.; Chilton, C. H. *Chemical Engineers' Handbook*; McGraw-Hill: New York, 1973.

(16) Atkins, P. W. *Physical Chemistry*, Oxford University Press: Oxford, 1982.

(17) Hidy, G. M. *Aerosols, An Industrial and Environmental Science*; Academic Press: Orlando, FL, 1984.

(18) Hanson, D. R.; Ravishankara, A. R. *J. Geophys. Res.* **1991**, *96*, 5081.

(19) Fehsenfeld, F. C.; Howard, C. J.; Schmeltekopf, A. L. *J. Chem. Phys.* **1975**, *63*, 2835.

(20) Bruins, A. P. *Mass. Spectrom. Rev.* **1991**, *10*, 53.

(21) Zhang, R.; Leu, M.-T.; Keyser, L. F. *Geophys. Res. Lett.* **1995**, *22*, 1493.

(22) Langhaar, H. L. *J. Appl. Mech.* **1942**, *9*, A55.

(23) Keyser, L. F. *J. Phys. Chem.* **1984**, *88*, 4750.

(24) Brown, R. L. *J. Res. Natl. Bur. Stand. (U.S.)* **1978**, *83*, 1.

(25) Fuchs, N. A.; Sutugin, A. G. *Highly Dispersed Aerosols*, Ann Arbor Science, Ann Arbor, MI, 1970.

(26) Patrick, R.; Golden, D. M. *Int. J. Chem. Kinet.* **1983**, *15*, 1189.

(27) Hirschfelder, J. O.; Curtiss, C. F.; Bird, R. B. *Molecular Theory of Gases and Liquids*; Wiley and Sons: New York, 1964.

(28) Tang, I. N. *Atmos. Environ.* **1980**, *14*, 819.

(29) Zhang, R.; Wooldridge, P. J.; Molina, M. J. *J. Phys. Chem.* **1993**, *97*, 8541.

(30) Van Doren, J. M.; Watson, L. R.; Davidovits, P.; Worsnop, D. R.; Zahniser, M.; Kolb, C. E. *J. Phys. Chem.* **1990**, *94*, 3265. Van Doren, J. M.; Watson, L. R.; Davidovits, P.; Worsnop, D. R.; Zahniser, M.; Kolb, C. E. *J. Phys. Chem.* **1991**, *95*, 1684.

(31) George, Ch.; Ponche, J. L.; Mirabel, Ph.; Behnke, W.; Scheer, V.; Zetzsch, C. *J. Phys. Chem.* **1994**, *98*, 8780.

(32) Robinson, G. N.; Worsnop, D. R.; Jayne, J. T.; Kolb, C. E.; Davidovits, P. *J. Geophys. Res.*, submitted, 1996.

(33) Tang, I. N.; Fung, K. H.; Imre, D. G.; Munkelwitz, H. R. *Aerosol Sci. Technol.* **1995**, *23*, 443.

(34) Cziczo, D.; Hu, J. H.; Nowak, J. B.; Abbatt, J. P. D. *J. Geophys. Res.*, submitted, 1997.